Kinetic Studies of FR-1, a Growth Factor-Inducible Aldo-Keto Reductase†

Sanjay Srivastava,‡ Theresa M. Harter,§ Animesh Chandra,‡ Aruni Bhatnagar,‡ Satish K. Srivastava,‡ and J. Mark Petrash*,§,||

Department of Human Biological Chemistry & Genetics, University of Texas Medical Branch, Galveston, Texas, and Departments of Ophthalmology & Visual Sciences and Genetics, Washington University School of Medicine, 660 South Euclid Avenue, Box 8096, St. Louis, Missouri 63110

Received February 24, 1998; Revised Manuscript Received May 28, 1998

ABSTRACT: Murine fibroblasts cultured in the presence of fibroblast growth factor-1 express relatively high levels of FR-1, a ∼36 kDa protein related to the aldo-keto reductase superfamily [Donohue, P. J., Alberts, G. F., Hampton, B. S., Winkles, J. A. (1994) *J. Biol. Chem. 269*, 8604−8609]. While the crystal structure of FR-1 shows striking homology with human aldose reductase [Wilson, D. K., Nakano, T., Petrash, J. M., Quiocho, F. A. (1995) *Biochemistry 34*, 14323−14330], an enzyme linked to the pathogenesis of diabetic complications, the physiological role of FR-1 is not known. We show that FR-1 is capable of reducing a broad range of aromatic and aliphatic aldehydes, including the abundant and highly reactive lipid-derived aldehyde 4-hydroxy-2-nonenal (HNE; $K_m \approx 9\ \mu$M). However, in the absence of coenzyme, HNE caused a time-dependent inactivation of FR-1. Results from electrospray ionization-mass spectrometry and Edman-degradation of peptides derived from HNE-modified FR-1 were consistent with formation of a Michael adduct at Cys298. This was confirmed with a C298S mutant, which was resistant to HNE-induced inactivation. Since steady-state K_m values determined with alkanals, α,β-unsaturated alkenals, alkadienals, and 4-hydroxyalkenals fall within their physiological concentrations, lipid-derived aldehydes appear to be potential in vivo substrates for FR-1.

Cell growth in response to peptide hormones involves coordinated expression of several cell cycle regulated genes. Initial stimulation leads to the expression of multiple immediate-early and delayed-early genes which probably modulate the transcription rates of target genes associated with subsequent DNA synthesis, mitosis, and cell division (*2*−*5*). While several immediate-early and delayed-early response gene products have been identified, in most cases, their contributions to cell cycle regulation remain obscure. One delayed-early gene product, designated FR-1, was recently identified on the basis of its marked upregulation following acidic growth factor-stimulation of quiescent murine fibroblasts (*2*). Sequencing studies demonstrated that FR-1 is a member of the aldo-keto reductase (AKR)[1] superfamily (*1*). The AKRs catalyze the reduction of a broad range of substrates including aldoses, aliphatic and aromatic aldehydes and ketones, steroids, prostaglandins, and xenobiotics such as chemotherapeutic drugs (*1*). In addition to FR-1, several AKRs have been identified in murine cells including aldose reductase (*6*) and MVDP, a testosterone-inducible protein abundant in mature vas deferens (*7*). Aldose reductase functions in vivo to convert glucose to sorbitol, an intermediate in the polyol pathway leading from glucose to fructose. A metabolic role for MVDP has not been reported to date although it has conserved the catalytic residues located at the active sites of other members of the AKR superfamily (*8*−*10*).

We previously showed that FR-1 adopts a $(\beta/\alpha)_8$ barrel structural motif typical of the AKRs and has enzymatic activity demonstrated by its ability to reduce carbonyls such as glyceraldehyde in the presence of NADPH (*11*). However, the physiological role of FR-1 is unknown. Because FR-1 is upregulated during early phase of the cell cycle, it is possible that this protein may be associated with the mitogenic activity of FGF-1 and related peptides. In the present study, we sought to determine if a particular structural class of substrates was used by FR-1 so as to indicate a potential physiological role for this enzyme.

† This work was supported in part by NIH Grants EY05856, P30EY02687, HL59378, DK20579, and DK36118. Additional support was provided by Research to Prevent Blindness, Inc. through a Lew R. Wasserman Merit Award (J.M.P.) and an unrestricted award to the Washington University Department of Ophthalmology and Visual Sciences.

* To whom correspondence should be addressed. Tel: (314) 362-1172. Fax: (314) 362-3638. E-mail: petrash@seer.wustl.edu.

‡ University of Texas Medical Branch.

§ Department of Ophthalmology & Visual Sciences, Washington University School of Medicine.

|| Department of Genetics, Washington University School of Medicine.

[1] Abbreviations: AKR, aldo-keto reductase; ALR2, aldose reductase; amu, atomic mass units; DTT, dithiothreitol; ESI-MS, electrospray ionization-mass spectrometry; FGF-1, fibroblast growth factor-1 or acidic fibroblast growth factor; FR-1, fibroblast growth factor I-regulated protein 1; HNE, 4-hydroxynonenal; MVDP, mouse vas deferens protein; PTH, phenylthiohydantoin; RP-HPLC, reversed-phase high-performance liquid chromatography; Sorbinil, [CP-45634; (*S*)-6-fluoro-spiro-[chroman-4, 4′-imidazolidine]-2′,5′-dione]; TFA, trifluoroacetic acid; Tolrestat, (AY-27773; *N*-[[5-(trifluoromethyl)-6-methoxy-1-naphthalenyl]thioxomethyl]-*N*-methylglycine); Zopolrestat, 3,4-dihydro-4-oxo-3-[[5-(trifluoromethyl)-2-benzothiazolyl]methyl]-1-phthalazineacetic acid.

S0006-2960(98)00433-4 CCC: $15.00
Published on Web 08/28/1998

MATERIALS AND METHODS

Materials. NADP, NADPH, DL-glyceraldehyde, and DTT were purchased from Sigma Chemical Co., St. Louis, MO. Sorbinil and Tolrestat were gifts from Pfizer Central Research (Groton, CT) and Wyeth-Ayrest (Princeton, NJ), respectively. 4-Hydroxy *trans*-2-pentenal, 4-hydroxy-*trans*-2-hexanal, and 4-hydroxy-*trans*-2-octenal were generous gifts of Dr. Brengt Mannervick (University of Stockholm, Sweden). HNE was synthesized as its dimethyl acetal from dimethyl acetal of fumaraldehyde as described previously (*12*). Free HNE was prepared by acid hydrolysis (pH 3.0) for 1 h at room temperature. The sodium salt of malonaldehyde was prepared by the method of Marnett and Tuttle (*13*). Briefly, tetraethoxypropane (1.1 g; 5 mmol) and Dowex 50 (5 g) were agitated in 10 mL of H_2O in a shaking waterbath for 30 min at 25 °C. The slurry was then titrated to pH 7.0 using 1 N NaOH. The Dowex 50 was filtered off and the filtrate was extracted with water-saturated ethyl acetate. The aqueous phase was lyophilized and the residue was dissolved in 1.5 mL of H_2O and passed through a Sephadex LH-20 (1.8 × 40 cm) column, preequilibrated with H_2O. Fractions (2.5 mL) were collected, and those fractions demonstrating an absorption maximum at 267 nm were pooled and lyophilized. The resulting residue was dissolved in a minimal amount of H_2O and crystallized as the sodium salt with acetone. NMR identified this material to be free MDA in solution form. Other aldehydes used in the study were purchased from Aldrich and used without further purification.

Enzyme Assays. Enzyme determinations were carried out in a 1.0 mL system containing 50 mM potassium phosphate, 100 mM potassium chloride, 0.1 mM EDTA, 0.15 mM NADPH, and 1.0 mM HNE or 10 mM DL-glyceraldehyde. The change in A_{340} was monitored using either a Gilford Response or Cary 1E spectrophotometer. Where indicated, enzyme was reduced by incubation with 0.1 M DTT at 37 °C for 1 h. Excess DTT was removed by passing the sample over a Sephadex G-25 desalting column that had been previously equilibrated with nitrogen or argon-saturated 0.1 M potassium phosphate, pH 7.0. Assays to measure the reaction in the direction of alcohol oxidation were carried out at pH 7.0 and 7.4 using 0.25 mM NADP and 0.5 mM 1,4-dihydroxynonene prepared by reduction of HNE with sodium borohydride. The aldehyde substrates were varied over a concentration range covering from 0.2 to 7−10 times the K_m of each aldehyde. Initial velocity was measured at 6−8 different concentrations of each substrate. Individual saturation curves used to obtain the steady-state kinetic parameters were fitted to a general Michaelis−Menten equation according to Cleland (*14*). In all cases, the best fit to the data was chosen on the basis of the standard error of the fitted parameter and the lowest value of σ, which is defined as the sum of squares of the residuals divided by the degrees of freedom. Assays to determine susceptibility of FR-1 to aldose reductase inhibitors were carried out at pH 7.0 in the direction of aldehyde reduction using 10 mM DL-glyceraldehyde as substrate and 0.5−0.7 nM enzyme.

Cloning, Mutagenesis, and Overexpression of Enzymes. Wild-type and mutant forms of murine FR-1 were obtained by overexpression in *Escherichia coli* essentially as described previously (*11*). Site-directed mutagenesis was carried out by a PCR method in the pAMP2 cloning system (Life Technologies, Gaithersburg, MD) to obtain the mutant containing Ser substituted for Cys298 (C298S). Coding sequences in both wild-type and mutant expression constructs were completely sequenced to verify their structures. Proteins were purified by a method described for human aldose reductase (*15*) except elution from chromatofocusing columns was accomplished with a salt gradient (0−1 M NaCl) rather than with a pH gradient. Bands that were visualized by staining SDS−polyacrylamide gels with either Coomassie Brilliant Blue R or Sypro-Red (Molecular Probes, Eugene, OR) indicated the enzymes used for these studies were greater than 95% pure.

Enzyme Modification by HNE. The reduced enzyme was incubated at 25 °C with 0−100 μM HNE in nitrogen-purged 0.1 M potassium phosphate, pH 7.0. Aliquots were removed at indicated time intervals to determine the enzyme activity at 25 °C using 60 mM DL-glyceraldehyde as substrate. In some experiments, immediately after the incubation, excess HNE was removed using a Sephadex G-25 desalting column. The time course of inactivation of the enzyme was analyzed using a two-exponential equation:

$$y = a_1 \exp^{-t/\tau_1} + a_2 \exp^{-t/\tau_2} \quad (1)$$

where y is the fractional remaining activity, t is the time, a_1 and a_2 are the preexponential factors, and τ_1 and τ_2 are the pseudo-first-order time constants for the inactivation of the enzyme. Data for HNE-inactivation in the presence of NADP were analyzed using a single-exponential equation:

$$y = a \exp^{-t/\tau} \quad (2)$$

Determination of HNE Binding Site. Reduced enzyme, 0.47 mg (13 nmol), was incubated for 1 h at 25 °C in a 1.5 mL solution containing 0.1 mM 4-[^{3}H]HNE [2 mCi/mmol; prepared as described previously (*12*)] and 100 mM phosphate, pH 7.0. The unbound radioactivity was removed by ultrafiltration using an Amicon 10 microconcentrator (M_r cut off 10 000). Solid urea was then added to the mixture to a final concentration of 6 M. After incubation for 1 h, the material was dialyzed against 1000 vol of 50 mM *N*-ethylmorpholine-acetate buffer, pH 8.0. The dialyzed enzyme was digested by adding trypsin (1:100, w/w) and the mixture was incubated at 37 °C. After 3 h, another aliquot of trypsin in the ratio 1:50 (w/w) was added and the digestion was allowed to proceed for another 4 h. Digested materials were stored at −20 °C.

The enzyme digest was subjected to RP-HPLC using an ODS C_{18} column (0.46 × 25 cm, Rainin), preequilibrated with 0.1% aqueous TFA. Peptides were eluted with a linear gradient from 0 to 60% acetonitrile containing 0.1% TFA at a flow rate of 1 mL/min for 90 min, using a Beckman Gold System 406 (Beckman Instruments). The eluate was monitored at 215 nm and was collected into 0.4 mL fractions. Aliquots from column fractions were assayed for radioactivity by liquid scintillation counting. Fractions containing radioactivity were used for Edman degradation using a gas-phase sequencer (Applied Biosystems model 475A). PTH-amino acid derivatives from each cycle of Edman degradation were identified using RP-HPLC by comparison with standards. Eluate fractions from each RP-HPLC cycle were collected and were assayed for radioactivity by scintillation

counting. The average repetitive yield for Edman degradation of the HNE-modified peptide was 95.4%.

Electrospray Ionization-Mass Spectrometry. Electrospray ionization-mass spectra were obtained on a Finnigan-TSQ70 (upgraded to TSQ700) triple quadrapole instrument with a Vestec electrospray ionization source and tapered fused silica capillary needle (50 μm internal diameter). Additives to the enzyme sample (DTT or HNE) were removed prior to analysis using a desalting column. Protein samples (~50 μg/mL) containing 5 mM ammonium acetate, 50% methanol, and 5% acetic acid were infused into the mass spectrometer source at a rate of 0.82 μL/min using a Harvard syringe pump. The spray voltage was set at 3.6 kV and nozzle voltage set at 250 V, with a repeller voltage of 10 V. A source temperature of 241 °C was used and source bath N2 was set at 2.4−2.7 psi. The Quad 3 was scanned from 600 to 200 amu/3 s, and 128 scans were averaged before data were acquired to a file. Spectra were acquired at the rate of 275 amu/s over the mass range of 10 000−40 000 Da. In all cases, standard errors in mass determinations for FR-1 ranged between 1.5 and 2.5 mass units, which was similar to the errors calculated with protein standards (apomyoglobin and bovine serum albumin) used to calibrate the instrument.

RESULTS

Substrate Specificity. Steady-state kinetic parameters for FR-1 measured with a variety of carbonyl substrates are given in Tables 1 and 2. All substrates that saturated the enzyme exhibited Michaelis−Menten kinetics in the concentration range studied. Aromatic and lipid-derived aliphatic aldehydes were excellent substrates, with K_m values in the low micromolar range for substituted aromatic aldehydes such as phenylacetaldehyde and *p*-nitrobenzaldehyde. Within a series of linear alkanals, the K_m values tended to decrease with increasing chain length. A similar tendency toward lower K_m values with increasing chain length was observed in a series of 2-alkenals and 4-hydroxy-2-alkenals. Introduction of an α,β-unsaturated bond tended to result in increased K_m values in aldehydes ranging between 3 and 6 carbons in length. Addition of a hydroxyl group at the fourth carbon resulted in a modest decrease in K_m in C5 and C6 2-alkenals. Similarly, small decreases in K_m were observed using 6- and 9-carbon dienals containing 2,4-trans double bonds. Kinetic constants for nonanal were essentially unchanged following addition of an α,β-unsaturated bond (nonenal) and a hydroxyl group at the fourth carbon (4-hydroxy-2-nonenal).

Polyhydroxylated substrates such as aldoses and ketoses were poor substrates as evidenced by K_m values ranging upward of 245 mM observed with D-glucuronate (Table 2). No measurable activity was observed with fructose and a variety of steroids containing D-ring ketones such as 17α-hydroxyprogesterone and pregnenolone. In comparison, the simple aromatic ketone acetophenone was a relatively good substrate (K_m of 2.4 mM). In terms of catalytic efficiencies, short-chain ketones such as acetone and butanone were more than 5000-fold less favorable substrates as compared to their corresponding alkyl aldehydes propanal and butanal. Glyoxal and methylglyoxal were reduced by FR-1, although their apparent K_m values were relatively high, whereas no reactivity could be detected with malonaldehyde. No reactivity could be detected when NADH was substituted for NADPH using HNE as substrate in the direction of aldehyde reduction. We were also unable to detect alcohol oxidation in

Table 1. Kinetic Constants for the Catalytic Reduction of Aliphatic and Aromatic Aldehydes by FR-1[a]

substrate	K_m (mM)	k_{cat} (min^{-1})	k_{cat}/K_m (mM^{-1} min^{-1})
aromatic aldehydes			
benzaldehyde*	0.100 ± 0.008	17.1	171
phenylglyoxal*	0.030 ± 0.002	31.2	1040
phenylacetaldehyde	0.021 ± 0.002	17.3	824
p-nitrobenzaldehyde*	0.018 ± 0.003	29.9	1661
alkanals			
propanal	2.90 ± 0.280	17.4	6
butanal*	0.562 ± 0.051	26.6	47
pentanal*	0.054 ± 0.005	19.7	365
hexanal*	0.006 ± 0.001	12.4	2067
nonanal*	0.009 ± 0.001	32.4	3682
dicarbonyls			
malonaldehyde	NMA		
glyoxal	23.0 ± 1.8	53.2	2
methylglyoxal	3.6 ± 0.06	59.6	16
trans-2-alkenals			
acrolein	5.0 ± 0.8	15.0	3
crotonaldehyde	5.0 ± 0.3	12.7	3
trans-pentenal	0.288 ± 0.01	14.3	50
trans-2-hexenal	0.200 ± 0.001	14.9	74
trans-2-nonenal	0.010 ± 0.001	19.8	2062
4-hydroxy-*trans*-2-alkenals			
4-hydroxy-*trans*-2-pentenal	0.073 ± 0.004	25.7	352
4-hydroxy-*trans*-2-hexenal	0.155 ± 0.007	17.1	110
4-hydroxy-*trans*-2-octenal	0.028 ± 0.001	19.7	709
4-hydroxy-*trans*-2-nonenal	0.009 ± 0.001	22.7	2494
trans,*trans*-2,4-alkadienals			
trans,*trans*-2,4-hexadienal*	0.126 ± 0.055	18.1	144
trans,*trans*-2,4-nonadienal*	0.010 ± 0.001	38.6	4021

[a] Homogeneous, recombinant FR-1 was reduced by incubating with 0.1 M DTT at 37 °C for 60 min. Excess DTT was removed by gel filtration. Kinetic parameters of the reduced enzyme were determined in nitrogen saturated 0.1 M phosphate buffer (pH 7.0) as described in the text. Kinetic parameters with the indicated (*) aldehydes were determined in the presence of 3−5% ethanol as cosolvent. This concentration had no significant effect on enzyme activity. NMA, no measurable activity.

Table 2. Kinetic Constants for the Catalytic Reduction of Hydroxyaldehydes, Ketones, and Steroids by FR-1[a]

substrate	K_m (mM)	k_{cat} (min^{-1})	k_{cat}/K_m (mM^{-1} min^{-1})
aldoses and ketoses			
DL-glyceraldehyde[b]	0.96 ± 0.07	21	22
D-glucuronate	245 ± 36	1.5	0.006
D-galactose	786 ± 112	6.1	0.008
D-xylose	248 ± 28	5.5	0.022
D-glucose	TR		
D-fructose	NMA		
ketones			
acetone	527 ± 72	0.8	0.001
butanone	148 ± 47	1.3	0.009
acetophenone	2.4 ± 1.0	8.7	3.6
steroids[c]			
17α-hydroxyprogesterone	NMA		
progesterone	NMA		
androstane-3,17-dione	NMA		
pregnenolone	NMA		

[a] Kinetic constants were measured at pH 7.0. NMA, no measurable activity; TR, trace activity not sufficiently high to determine kinetic constants. [b] K_m of D-glyceraldehyde was 0.99 ± 0.15 mM. For other conditions see legend to Table 1. [c] Steroids were assayed in the presence of 5% ethanol as cosolvent. This concentration had no significant effect on enzyme activity.

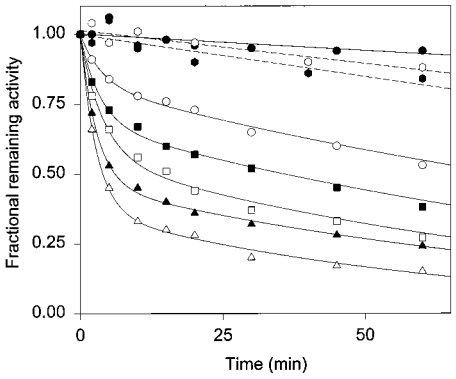

FIGURE 1: Inactivation of FR-1 by HNE. The reduced wild-type enzyme (1 μM) was incubated without (●) or with HNE at a final concentration of 10 μM (○), 20 μM (■), 40 μM (□), 75 μM (▲), and 100 μM (△). Also shown are data for the C298S mutant of FR-1 incubated in the absence (⬡) and presence (⬢) of 100 μM HNE. For both wild-type and C298S, reductase activity was determined using 60 mM DL-glyceraldehyde on aliquots of the incubation mixture withdrawn at the indicated time intervals.

the presence of NADP using dihydrononenol (0.5 mM) as substrate. FR-1 was sensitive to aldose reductase inhibitors of the carboxylic acid category, as evidenced by low IC_{50} values measured with Tolrestat (134 ± 14 nM) and Zopolrestat (71 ± 5 nM). Its sensitivity to the spirohydantoin inhibitor Sorbinil (IC_{50} = 42 ± 8 μM) was 2−3 orders of magnitude lower as compared to the carboxylic acids.

Inactivation of FR-1 by HNE. In contrast to its behavior as a substrate in the presence of NADPH, HNE caused a time- and concentration-dependent inactivation of the apoenzyme. Approximately 75% of the initial activity was lost when the enzyme was exposed to 40 μM HNE at pH 7.0 and 25 °C for 60 min (Figure 1), and no measurable activity was observed after incubating the enzyme with 250 μM HNE for 60 min at 25 °C. The rate of inactivation was well described by a biexponential function. The observed rate constants and the intercept values obtained from the best fits of eq 1 are listed in Table 3. These data indicate that HNE causes a rapid initial phase of inactivation followed by a subsequent slower phase of inactivation. Since the initial rate of inactivation (τ_1) was constant over the concentration range studied, it appears this phase of inactivation is due to high-affinity binding of HNE to the enzyme, which is followed by a slower phase (τ_2) of modification of the enzyme (Table 3). A replot of the observed rates of inactivation ($1/\tau_2$) displayed a hyperbolic dependence on HNE concentration (data not shown) consistent with the formation of a dissociable complex between the enzyme and HNE before irreversible inactivation.

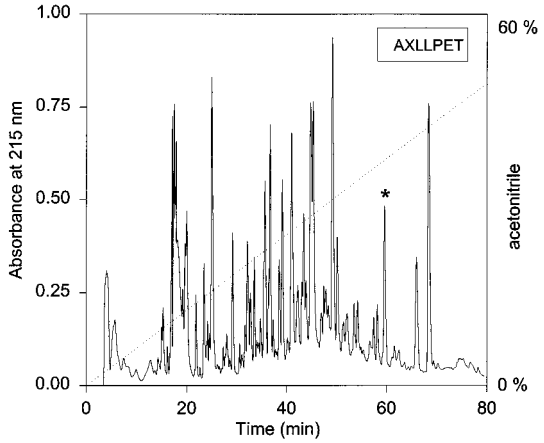

FIGURE 2: Reversed-phase HPLC of trypsin digest of 3H-[HNE]-modified FR-1. Tryptic fragments produced from HNE-modified FR-1 were resolved by RPHPLC as described in the text. Radioactivity was measured by scintillation counting of aliquots (5 μL) taken from each 0.4 mL column fraction. The only fractions containing radioactivity ≥2 times background were associated with the peak indicated by the asterisk (∗). (Inset) The sequence of the peptide eluting at ∼60 min was determined by Edman degradation. Since no identifiable PTH-amino acid derivative was observed in cycle 2, this position in the sequence is shown as "X".

In addition to HNE, the enzyme was inactivated by other unsaturated aldehydes. Incubation of the enzyme with 100 μM each of 4-hydroxyoctenal and *trans*-2-nonenal led to a complete loss of enzyme activity in 60 min. In contrast, the enzyme appeared to be insensitive to saturated aldehydes, since no significant loss of enzyme activity was observed upon incubation with 100 μM nonanal for 60 min. NADP protected the enzyme against HNE-induced loss of enzyme activity, and the time constant for inactivation of FR-1 was very long (>300 min) in the presence of both 40 μM HNE and 50 μM NADP (Table 3).

To probe the HNE binding site on FR-1, we incubated FR-1 with 4-[^{3}H]HNE and resolved a radiolabeled tryptic peptide by RP-HPLC (Figure 2). This peptide was then subjected to sequential Edman degradation, which yielded the following sequence: NH_2-Ala-unidentified-Leu-Leu-Pro-Glu-Thr-COOH. This peptide sequence aligns with the FR-1 primary sequence at positions 297−303, where the unidentified residue in the second cycle of Edman degradation would correspond to Cys298 of FR-1.

Previous studies have shown that HNE covalently modifies proteins through Cys residues (*16*). FR-1 contains six Cys residues, four of which are located at positions homologous to human aldose reductase (*2*, *11*), including Cys298. This residue in human aldose reductase is reported to play an

Table 3. Inactivation of FR-1 by HNE[a]

additives	parameters				
	a_1	τ_1	a_2	τ_2	R^2
10 μM HNE	0.18 ± 0.02	3.81 ± 1.1	0.82 ± 0.02	149.4 ± 11.1	0.9997
20 μM HNE	0.31 ± 0.03	3.47 ± 0.74	0.68 ± 0.02	114.4 ± 10.8	0.9994
40 μM HNE	0.43 ± 0.04	4.10 ± 0.91	0.56 ± 0.04	90.3 ± 13.7	0.9985
100 μM HNE	0.63 ± 0.02	2.80 ± 0.22	0.37 ± 0.02	63.0 ± 6.3	0.9993
40 μM HNE + 50 μM NADP	1.04 ± 0.02	375.1 ± 78.2			0.9988

[a] Reduced FR-1 was incubated with the indicated concentrations of the additives in nitrogen-purged 0.1 M potasium phosphate (pH 7.0). Aliquots were removed at specified time intervals (see Figure 1) and assayed for enzyme activity. The parameters were calculated from the best fits of eq 1 to the data for HNE, and eq 2 for HNE + NADP.

Table 4. Kinetic Constants for the C298S Mutant of FR-1[a]

substrate	K_m (mM)	k_{cat} (min^{-1})	k_{cat}/K_m (mM^{-1} min^{-1})	k_{cat} C298S/WT	k_{cat}/K_m C298S/WT
DL-glyceraldehyde	5.1 ± 0.4	73.7	14.4	3.5	0.65
D-xylose	618 ± 52	17.2	0.03	3.1	1.3
hexanal	0.16 ± 0.021	36.5	228	2.9	0.11
p-nitrobenzaldehyde	0.045 ± 0.005	72.1	1602	2.5	0.96
4-hydroxy-*trans*-2-pentenal	0.404 ± 0.012	27.5	68	1.1	0.19
4-hydroxy-*trans*-2-hexenal	1.11 ± 0.072	21.2	19	1.2	0.17
4-hydroxy-*trans*-2-octenal	0.354 ± 0.010	37.2	105	1.8	0.15
4-hydroxy-*trans*-2-nonenal	0.042 ± 0.002	36.2	862	1.6	0.35
nonanal	0.033 ± 0.004	46.1	1398	1.4	0.37
trans-2-nonenal	0.063 ± 0.006	29.2	464	1.4	0.23
trans,*trans*-2,4-nonenal	0.042 ± 0.004	61.3	1460	1.5	0.36

[a] For experimental conditions see legend to Table 1.

important role in regulating the catalytic rate and binding affinity to some aldose reductase inhibitors (*15*, *17*). To confirm that HNE inactivates FR-1 by modifying Cys298, we measured the susceptibility to HNE-inactivation of a mutant containing a Ser substituted for Cys298 (C298S). As shown in Figure 1, the C298S mutant was resistant to inactivation when incubated in the presence of 100 μM HNE for 60 min. In contrast, the wild-type FR-1 control lost over 75% of starting activity when incubated under identical conditions. It is unlikely that the apparent resistance to HNE inactivation was due to major reorganization of the FR-1 structure since the catalytic efficiencies of the C298S mutant measured with a variety of substrates were altered by less than 1 order of magnitude relative to wild-type FR-1 (Table 4). In general, the C298S mutant form of FR-1 displayed higher K_m values for the aldehyde substrates and a slightly reduced catalytic efficiency and as compared to the wild-type enzyme. As reported for the C298S mutant of human aldose reductase, the FR-1 C298S mutant displayed higher k_{cat} values for short-chain and aromatic aldehydes as compared to the wild-type enzyme (*15*). In contrast, the k_{cat} values measured with long-chain alkenals and alkanals were essentially unaffected by the C298 substitution (Table 4).

Electrospray ionization-mass spectrometry (ESI-MS) was used to characterize the reaction products of HNE-treatment of FR-1. As shown in Figure 3, the spectrum of the untreated control FR-1 contained a well-defined peak corresponding to a molecular mass of 35 989.5 Da. This value agrees well with the molecular mass of 35 989.4 Da predicted from the protein primary sequence. Analysis of the reaction mixture containing FR-1 modified by incubation with 75 μM HNE revealed two prominent species corresponding to molecular mass of 35 984.9 and 36 143.0 Da (Figure 3B). The difference in mass between these species (158.1 Da) agrees well with the theoretical prediction for addition of 1 mol of HNE (156 Da) to FR-1. Similar analysis of the C298S mutant following treatment with HNE revealed a single species with a mass (35 972.8 Da), which is essentially identical to that of the untreated C298S control (35 971.2 Da; see Figure 3, panels C and D).

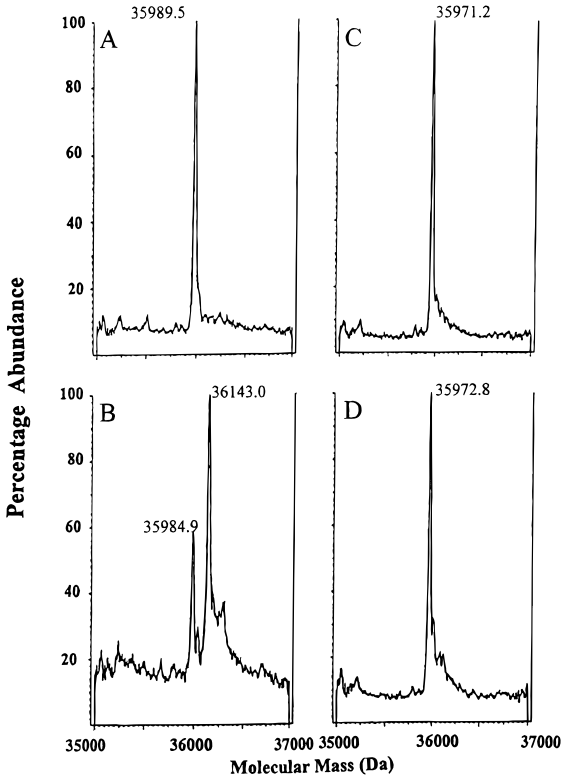

FIGURE 3: Electrospray ionization-mass spectrometry of FR-1. Enzymes were incubated with or without HNE (75 μM) for 1 h, followed by rapid desalting by gel filtration in nitrogen saturated ammonium acetate. (A) Native FR-1; (B) FR-1 treated with HNE; (C) Native C298S mutant of FR-1; (D) C298S mutant of FR-1 treated with HNE.

DISCUSSION

The aldo-keto reductases (AKR) comprise a superfamily of proteins presently grouped according to amino acid and nucleotide sequence similarities into one of at least seven families designated AKR1 through AKR7[2] (*1*). On the basis of high sequence identity (>70%) with various prototypical aldo-keto reductases (*2*), FR-1 has been placed into the AKR1 family where it has been assigned the designation AKR 1B8 (*1*).

High-resolution crystal structures of human aldose reductase holoenzyme and the ternary complex containing various active-site inhibitors have provided structural insights into ligand-binding domains that are most likely shared by many members of the AKR superfamily (*18*−*21*). Like other AKRs where structures are available, FR-1 adopts a $(\beta/\alpha)_8$ barrel structure characterized by a deep hydrophobic active-

[2] Current members of the aldo-keto reductase superfamily can be seen on the AKR WEB page at http://pharme26.med.upenn.edu. According to the nomenclature system proposed by Jez et al. (*1*), FR-1 is equivalent to AKR 1B8.

site located near the C-terminal end of the β-barrel (*11*). The coenzyme binds with the nicotinamide ring situated at the base of the active-site cavity, with the pyrophosphate straddling the top of the barrel, and the adenosine fits into a cavity on the edge. Zopolrestat binds in the active site and is stabilized by numerous interactions involving hydrophobic residues. The carboxylate group of the inhibitor interacts with His110 and Tyr48 of FR-1 in a manner proposed to be similar to other AKRs complexed with carbonyl substrates (*11*, *18*, *19*).

Our observations show that FR-1 is capable of reducing carbonyls derived from a broad range of structural classes including both aromatic and aliphatic aldehydes. However, relatively poor reactivity was observed with short-chain ketones such as acetone and butanone. In contrast, the catalytic efficiency that was observed with the aromatic ketone acetophenone was almost 3 orders of magnitude greater. FR-1 was weakly active with aldoses such as glucose, galactose, and xylose, clearly indicating that the enzyme probably plays little, if any role in hexose metabolism in vivo. Because FR-1 did not catalyze the oxidation of the cognate alcohols, its primary catalytic role is probably that of an aldehyde reductase.

In addition to the inability to catalyze glucose reduction, several kinetic features distinguish FR-1 from aldose reductase. As we reported previously (*11*), FR-1 has a significantly higher K_m for DL-glyceraldehyde (1.0 mM) than for aldose reductase (0.05 mM). Like bovine lens aldose reductase (*22*), FR-1 does not appear to significantly discriminate between L- and D-isoforms of glyceraldehyde, since its K_m values for D-glyceraldehyde and DL-glyceraldehyde were essentially the same (Table 2). In addition, FR-1 catalyzes the reduction of ketones. In contrast, aldose reductase displays high selectivity toward the aldehydic carbonyl (*23*) although reduction of the ketone carbonyls of methylglyoxal (*24*) and 17α-hydroxyprogesterone (*25*) have been reported. Interestingly, the K_m of FR-1 for methylglyoxal (4 mM) is much higher than that reported for aldose reductase (8 μM) (*24*). Reasons for low affinity of FR-1 for methylglyoxal are not known, but may relate to the larger active site of FR-1 (*11*) that may provide less efficient binding for trioses. This may be the case for other short-chain aldehydes as well. The K_m of FR-1 for acrolein is 5 mM compared to 80 μM for aldose reductase (*26*), and the reduction of malonaldehyde is not catalyzed by FR-1 at all. In contrast to that reported for aldose reductase (*23*, *27*), the oxidation state of the α-carbon does not appear to be a significant determinant of substrate specificity of FR-1. The K_ms for the C3 aldehydes propanal and methylglyoxal were similar (3 and 4 mM, respectively), irrespective of the different oxidation states of their α-carbons.

Unlike aldose reductase, which is genetically identical to mammalian 20α-hydroxysteroid dehydrogenase (*28*), FR-1 was essentially inactive with the naturally occurring steroids 17α-hydroxyprogesterone and pregnenolone. Functional divergence from aldehyde reductase (glucuronate reductase) was evident by the poor utilization of glucuronate by FR-1 and by the high sensitivity of FR-1 to the aldose reductase inhibitors examined in this study. In addition, our studies with FR-1 demonstrate that the K_m values measured with various long-chain alkanals are at least 2 orders of magnitude lower than corresponding data reported for aldehyde reductase (*29*). In some respects, the substrate specificity of FR-1 overlaps that of CHO reductase, an AKR induced in Chinese hamster ovary cells following culture in the presence of a peptide aldehyde (*N*-acetyl-leucyl-leucyl-norleucinal) (*30*, *31*). Both FR-1 and CHO reductase catalyze the reduction of benzaldehyde and *p*-nitrobenzaldehyde with similar efficiency. However, despite a high degree of amino acid sequence identity between the two enzymes (92%), large differences (>10-fold) in apparent K_m values are evident with other substrates such as DL-glyceraldehyde and phenylglyoxal. It seems likely that CHO reductase and FR-1 represent orthologous gene products since their sequences are almost identical in the C-terminal region, which is known to be hypervariable among members of the AKR superfamily. It is possible that the kinetic differences between CHO reductase and FR-1 might be manifestations of the $(His)_6$ leader sequence added to the N-terminus of recombinant CHO reductase to aid in its expression and purification (*31*). Recombinant FR-1 used in the present study was produced without a fusion sequence at either end of the protein.

Among all substrates investigated in the present study, alkanals and α,β-unsaturated alkenals, alkadienals, and 4-hydroxyalkenals with a large hydrocarbon side chain appear to be the best physiological substrates. Within a homologous series, the catalytic efficiency increased with an increase in carbon chain length. For alkanals, the K_m decreased more than 400-fold as the hydrocarbon chain length increased from C3 to C6. A similar trend was observed with the trans-2 alkenals and the 4-hydroxy trans-2 alkenals, indicating that FR-1 preferentially catalyzes the reduction of long-chain aldehydes. This pattern of substrate specificity may relate to the greater extent to which long-chain aldehydes could interact with hydrophobic residues that line the active site. Comparison of the saturated and unsaturated aldehydes shows that alkanals up to C6 have a lower K_m than their corresponding α,β-alkenals, presumably due to the greater flexibility of alkanals over the trans-2 alkenals. However, no further enhancement of catalytic efficiency was observed on increasing the number of double bonds (the trans,trans-2,4-alkadienals were reduced with similar efficiency), indicating that constraints at C2 (α-carbon) are more likely to affect catalysis than those at C4. The insensitivity of catalysis to C4 substituents is further evidenced by comparable kinetic constants for 4-hydroxy-trans-2 alkenals and trans-2-alkenals.

Saturated aldehydes up to C6 had a lower K_m than their corresponding α,β-alkenals. However, addition of an α,β double bond had little effect on the catalytic efficiency for the C9 alkanal, nonanal. Introduction of an additional double bond between carbons 4 and 5 or a hydroxyl group at the fourth carbon of C6 and C9 alkenals did not appear to affect the steady-state kinetic parameters.

Like long-chain aliphatic aldehydes, aromatic aldehydes were also found to be excellent substrates for FR-1. This is consistent with predictions from structural modeling of the FR-1 holoenzyme complexed with zopolrestat, which revealed extensive stabilization of the inhibitor's aromatic rings by numerous hydrophobic amino acid side chains lining the active site (*11*). Since crystal structures for aldose reductase holoenzyme complexed with active-site inhibitors demonstrated extensive stabilization through hydrophobic interactions (*18*, *19*), it seems likely that the low K_m values we

observe with the variety of hydrophobic substrates examined in this study reflect stabilization by similar interactions in FR-1.

Incubation of the apoenzyme with micromolar concentrations of HNE led to a time- and concentration-dependent inactivation of the enzyme. However, HNE-induced modification of FR-1 was inhibited by NADP, suggesting that the modification site overlapped the coenzyme binding site or became masked as a result of a conformational change induced by coenzyme binding (*32*, *33*). The rate of inactivation showed a biexponential time course, which is suggestive of two discrete inactivation processes. Amino acid sequencing of 4-[^{3}H]HNE-modified FR-1, coupled with ESI-MS measurements which show equimolar binding of HNE to FR-1, demonstrate that Cys298 is the predominant site of HNE modification. This conclusion is also supported by the observation that the C298S mutant was resistant to inactivation by HNE. Thus, the biexponential inactivation rate does not appear to be due to modification of two distinct sites on the enzyme. Instead, we postulate an inactivation process involving rapid binding of HNE to the hydrophobic active site followed by a slow conformational change, which leads to complete inactivation. The ESI-MS data indicate that inactivation of FR-1 occurs through formation of a Michael adduct with Cys298 rather than Schiff base formation with lysine or histidine residues. The protective effect of NADP suggests that in the presence of coenzyme, the rate of HNE modification of the enzyme will be substantially reduced. In light of the strong binding affinity of FR-1 for NADPH and NADP (K_d equals 0.45 and 0.23 μM, respectively) (*11*), the enzyme can be expected to exist in vivo mainly as the holoenzyme. Therefore, reduction of α,β-unsaturated aldehydes by FR-1 should not be limited by substrate modification and/or nonspecific oxidation of the enzyme except under highly oxidizing conditions.

Similar to earlier observations with aldose reductase (*15*, *17*, *34*), Cys298 appears to play a potential modulatory role in FR-1. Modification studies with HNE suggest that the nucleophilicity of this residue (i.e., its reactivity with α,β-unsaturated aldehydes) is similar to the corresponding cysteine in aldose reductase (*34*). While substitution of Cys298 with serine in aldose reductase causes large changes in K_m of DL-glyceraldehyde, xylose, and *p*-nitrobenzaldehyde (54-, 54.3-, and 13-fold, respectively), relatively smaller changes were observed when a similar substitution was made in FR-1 (corresponding K_m values were increased by 5.3-, 2.5-, and 2.5-fold, respectively). Moreover, no large changes in kinetic constants with substrates such as *p*-nitrobenzaldehyde were observed between the reduced and nonreduced FR-1. Turnover numbers were also found to be elevated in the C298S mutants of both aldose reductase and FR-1, although the increases tended to be more pronounced for aldose reductase when measured with DL-glyceraldehyde, xylose, and *p*-nitrobenzaldehyde (compare 3.5-, 6.8-, and 7.1-fold increases for aldose reductase versus 3.5-, 3.1-, and 2.5-fold increases for FR-1). The decrease in k_{cat}/K_m were also less dramatic with the C298S mutant of FR-1 as compared to aldose reductase. Thus, it appears that Cys298 plays a more important role in substrate binding and catalysis in aldose reductase than in FR-1. This may be a reflection of the fact that the distance between Cys298-Sγ to the C4 of the NADPH is less than 4 Å in aldose reductase (holoenzyme and ternary complex with inhibitor) whereas the corresponding distance in the FR-1 ternary complex is much longer (>7 Å) (*11*). Therefore, a potential role for Cys298 in stabilizing the closed conformation of the binary enzyme−coenzyme complex in aldose reductase may not be directly applicable to Cys298 in FR-1 (*17*).

Lipid-derived aldehydes formed in tissues as a result of oxidation of lipids by reactive oxygen species are highly reactive organic compounds characterized by the presence of a polarizable carbonyl group (*35*). The carbonyl carbon is an electrophilic site and can easily react with nucleophiles such as amines. With α/β-unsaturation, the molecule becomes much more reactive as a result of the β-carbon conjugation with the carbonyl group. This causes the β-carbon to become positively polarized and, therefore, a potential site of nucleophilic attack. The partial positive charge can be further influenced by substituents such as a hydroxyl group at C4. Consequently, 4-hydroxyalkenals react avidly with nucleophiles such as histidine, lysine, and thiols via a Michael-type nucleophilic addition (*35*, *36*). These aldehydes and their derivatives have been suggested to play a critical role in several disease states and aging (*36*, *37*). Protein adducts of such aldehydes are generated during oxidation of low-density lipoprotein (*38*) and have been localized to atherosclerotic plaques of humans and animals (*39*) as well as to lesions in neurons of patients with Alzheimer's (*40*) and Parkinson diseases (*41*). In addition, high concentrations of aldehyde-derived DNA adducts have been found not only in animals exposed to carcinogens, but also in humans and animals even without carcinogen treatment (*42*). This suggests that these adducts may represent common background DNA lesions related to spontaneous carcinogenesis and aging. Because reduction removes the α,β-unsaturation, it markedly reduces the reactivity of these aldehydes, and thus FR-1-mediated catalysis may be a part of the cellular defenses against oxidative stress.

The most likely sources of long-chain hydrophobic and α,β-unsaturated aldehydes are lipid peroxidation reactions (*35*). Radical-mediated peroxidative reactions of unsaturated lipids leads to the generation of the reactive alkoxyl radical, which upon spontaneous radical elimination (β-scission) generates several saturated and unsaturated aldehydes (*43*). With ω-6 polyunsaturated fatty acids (arachidonate, linolenate, linoleate), the most abundant aldehydes generated are the 4-hydroxyalkenals. Because these aldehydes are highly reactive and are generated in high concentrations, it has been suggested that they mediate and amplify the cellular effects of their radical precursors (*35*). Significant quantities of these aldehydes may also be formed by other metabolic processes such as myeloperoxidase-catalyzed oxidation of amino acids (*44*), oxidative modification of nucleosides (*45*) and polyamine metabolism (*46*). Furthermore, α,β-unsaturated aldehydes are produced during metabolism of several drugs, toxicants and foods, and are ubiquitous components of pollutants (*16*). Our studies demonstrate that the kinetic properties of FR-1 are consistent with a potential in vivo role for this enzyme in metabolism of hydrophobic aldehydes.

High concentrations of aldehydes are generated under conditions of oxidative stress. Lipid peroxidation of rat liver microsomes results in the accumulation of hydroxyalkenals in the lipid membrane of the order of 100 mM (*47*).

Estimates of lipid aldehyde concentration in the liver of rats intoxicated with haloalkanes range from 4 to 11 mM, and even during early states of lipid peroxidation, the expected HNE concentration in the lipid bilayer was estimated to be 4.5 mM (*48*). While the exact partition coefficient of HNE between the cytoplasm and the membrane lipids is not known, its partition coefficient between water and chloroform is 0.04 (*49*). Using this value, the expected concentration of HNE in the cytoplasm during lipid peroxidation may be 200−400 μM. However, because HNE and related aldehydes are highly reactive and rapidly metabolized, their steady-state concentrations are expected to be in the low micromolar range. It has been reported that the normal human plasma contains 1−3 μM HNE (*50*), and under pathological conditions such as hypovolumic shock or vitamin E deficiency, plasma HNE concentrations elevated to 2−40 μM have been measured (*35*). Because the K_m of FR-1 is within the range of aldehyde concentrations measured under physiological and pathological conditions and since reduction diminishes the reactivity of these aldehydes by removing α,β-unsaturation, metabolism of lipid-derived aldehydes by FR-1 may represent an important part of the cellular defenses against oxidative stress.

Induction of FR-1 during the early phases of mitogenic signaling is also consistent with its potential role in lipid metabolism. Recent evidence suggests that stimulation of cells by several growth factors results in enhanced production of reactive oxygen species associated with cell cycle progression and $p21^{ras}$-mediated signaling (*51*−*53*). Although the specific signaling events involved have not been elucidated, high concentrations of reactive oxygen species generated in response to mitogens may lead to enhanced production of lipid-derived aldehydes. FR-1, also upregulated during this phase, may serve to contain the toxicity of lipid-derived aldehydes produced by reactive oxygen species and thus facilitate cell growth.

It is possible that FR-1 contributes to the enzymatic capacity reported previously for pyridine nucleotide-dependent reduction of lipid-derived aldehydes in the cytosolic fraction of a mouse fibroblast cell line (*54*). A correlation between the length and degree of saturation of the carbon chain and toxicity of the α,β-unsaturated aldehydes toward human fibroblasts has also been observed, with the rank order of toxicity as follows: hexenal < nonenal < nonadienal < hydroxynonenal. Since K_m values for these compounds fall within the range of their physiological concentrations, it would appear that FR-1 is well suited to function as a detoxifying enzyme toward these naturally occurring aldehydes.

ACKNOWLEDGMENT

The skillful assistance of Terry Griest and Jen Chyong-Wang is gratefully acknowledged.

REFERENCES

1. Jez, J. M., Flynn, T. G., and Penning, T. M. (1997) *Adv. Exp. Med. Biol. 414*, 579−600.
2. Donohue, P. J., Alberts, G. F., Hampton, B. S., and Winkles, J. A. (1994) *J. Biol. Chem. 269*, 8604−8609.
3. Breyer, J. A. (1997) *Sem. Nephrol. 17*, 114−123.
4. Imamura, T., Engleka, K., Zhan, X., Tokita, Y., Forough, R., Roeder, D., Jackson, A., Maier, J. A., Hla, T., and Maciag, T. (1990) *Science 249*, 1567−1570.
5. Gay, C. G., and Winkles, J. A. (1990) *J. Biol. Chem. 265*, 3284−3292.
6. Gui, T., Tanimoto, T., Kokai, Y., and Nishimura, C. (1995) *Eur. J. Biochem. 227*, 448−453.
7. Pailhoux, E. A., Martinez, A., Veyssiere, G. M., and Jean, C. G. (1990) *J. Biol. Chem. 265*, 19932−19936.
8. Tarle, I., Borhani, D. W., Wilson, D. K., Quiocho, F. A., and Petrash, J. M. (1993) *J. Biol. Chem. 268*, 25687−25693.
9. Barski, O. A., Gabbay, K. H., Grimshaw, C. E., and Bohren, K. M. (1995) *Biochemistry 34*, 11264−11275.
10. Bennett, M. J., Schlegel, B. P., Jez, J. M., Penning, T. M., and Lewis, M. (1996) *Biochemistry 35*, 10702−10711.
11. Wilson, D. K., Nakano, T., Petrash, J. M., and Quiocho, F. A. (1995) *Biochemistry 34*, 14323−14330.
12. Chandra, A. and Srivastava, S. K. (1997) *Lipids 32*, 779−82.
13. Marnett, L. J., and Tuttle, M. A. (1980) *Cancer Res. 40*, 276−282.
14. Cleland, W. W. (1979) *Methods Enzymol. 63*, 103−138.
15. Petrash, J. M., Harter, T. M., Devine, C. S., Olins, P. O., Bhatnagar, A., Liu, S. Q., and Srivastava, S. K. (1992) *J. Biol. Chem. 267*, 24833−24840.
16. Witz, G. (1989) *Free Radical Biol. Med. 7*, 333−349.
17. Grimshaw, C. E., Bohren, K. M., Lai, C. J., and Gabbay, K. H. (1995) *Biochemistry 34*, 14366−14373.
18. Wilson, D. K., Tarle, I., Petrash, J. M., and Quiocho, F. A. (1993) *Proc. Natl. Acad. Sci. U.S.A. 90*, 9847−9851.
19. Urzhumtsev, A., Tetefavier, F., Mitschler, A., Barbanton, J., Barth, P., Urzhumtseva, L., Biellmann, J. F., Podjarny, A. D., and Moras, D. (1997) *Structure 5*, 601−612.
20. Harrison, D. H., Bohren, K. M., Ringe, D., Petsko, G. A., and Gabbay, K. H. (1994) *Biochemistry 33*, 2011−2020.
21. El-Kabbani, O., Judge, K., Ginell, S. L., Myles, D. A., DeLucas, L. J., and Flynn, T. G. (1995) *Nat. Struct. Biol. 2*, 687−692.
22. Liu, S. Q., Bhatnagar, A., and Srivastava, S. K. (1992) *Biochim. Biophys. Acta 1120*, 329−336.
23. Kotecha, J. A., Feather, M. S., Kubiseski, T. J., and Walton, D. J. (1997) *Carbohydr. Res. 289*, 77−89.
24. Vander Jagt, D. L., Robinson, B., Taylor, K. K., and Hunsaker, L. A. (1992) *J. Biol. Chem. 267*, 4364−4369.
25. Pineda, J. A., Murdock, G. L., Watson, R. J., and Warren, J. C. (1989) *J. Steroid Biochem. 33*, 1223−1228.
26. Kolb, N. S., Hunsaker, L. A., and Vander Jagt, D. L. (1994) *Mol. Pharmacol. 45*, 797−801.
27. Vander Jagt, D. L., Kolb, N. S., Vander Jagt, T. J., Chino, J., Martinez, F. J., Hunsaker, L. A., and Royer, R. E. (1995) *Biochim. Biophys. Acta 1249*, 117−126.
28. Warren, J. C., Murdock, G. L., Ma, Y., Goodman, S. R., and Zimmer, W. E. (1993) *Biochemistry 32*, 1401−1406.
29. Matsuura, K., Deyashiki, Y., Bunai, Y., Ohya, I., and Hara, A. (1996) *Arch. Biochem. Biophys. 328*, 265−271.
30. Inoue, S., Sharma, R. C., Schimke, R. T., and Simoni, R. D. (1993) *J. Biol. Chem. 268*, 5894−5898.
31. Hyndman, D. J., Takenoshita, R., Vera, N. L., Pang, S. C., and Flynn, T. G. (1997) *J. Biol. Chem. 272*, 13286−13291.
32. Wilson, D. K., Bohren, K. M., Gabbay, K. H., and Quiocho, F. A. (1992) *Science 257*, 81−84.
33. Borhani, D. W., Harter, T. M., and Petrash, J. M. (1992) *J. Biol. Chem. 267*, 24841−24847.
34. Srivastava, S., Chandra, A., Ansari, N. H., Srivastava, S. K., and Bhatnagar, A. (1998) *Biochem. J. 329*, 469−475.
35. Esterbauer, H., Schaur, R. J., and Zollner, H. (1991) *Free Radical Biol. Med. 11*, 81−128.
36. Mattson, M. P., Mark, R. J., Furukawa, K., and Bruce, A. J. (1997) *Chem. Res. Toxicol. 10*, 507−517.
37. Stadtman, E. R., and Berlett, B. S. (1997) *Chem. Res. Toxicol. 10*, 485−494.
38. Foppiano, M., and Lombardo, G. (1997) *Lancet 349*, 399−400.
39. Yla-Herttuala, S., Palinski, W., Rosenfeld, M. E., Parthasarathy, S., Carew, T. E., Butler, S., Witztum, J. L., and Steinberg, D. (1989) *J. Clin. Invest. 84*, 1086−1095.

40. Sayre, L. M., Zelasko, D. A., Harris, P. L., Perry, G., Salomon, R. G., and Smith, M. A. (1997) *J. Neurochem. 68*, 2092−2097.
41. Yoritaka, A., Hattori, N., Uchida, K., Tanaka, M., Stadtman, E. R., and Mizuno, Y. (1996) *Proc. Natl. Acad. Sci. 93*, 2696−2701.
42. Chen, P., Wiesler, D., Chmelik, J., and Novotny, M. (1996) *Chem. Res. Toxicol. 9*, 970−979.
43. Grosch, W. (1987) in *Autoxidation of Unsaturated Lipids* (Chan, H. W. S., Ed.) pp 95−139, Academic Press, London.
44. Jacobi, G. H., Moore, R. J., and Wilson, J. D. (1977) *J. Steroid Biochem. 8*, 719−723.
45. Pfeifer, M. A., Schumer, M. P., and Gelber, D. A. (1997) *Diabetes 46*, Suppl. 2, S82−S89.
46. Ambroziak, W., and Pietruszko, R. (1991) *J. Biol. Chem. 266*, 13011−13018.
47. Benedetti, A., Comporti, M., Fulceri, R., and Esterbauer, H. (1984) *Biochim. Biophys. Acta* 172−181.
48. Koster, J. F., Slee, R. G., Montfoort, A., Lang, J., and Esterbauer, H. (1986) *Free Radic. Biol. Med. 1*, 273−287.
49. Esterbauer, H., and Weger, W. (1967) *Monatsh. Chem. 98*, 1994−2000.
50. Strohmaier, H., Hinghofer-Szalkay, H., and Schaur, R. J. (1995) *J. Lipid Mediat. Cell Signal. 11*, 51−61.
51. Sundaresan, M., Yu, Z. X., Ferrans, V. J., Irani, K., and Finkel, T. (1995) *Science 270*, 296−299.
52. Irani, K., Xia, Y., Zweier, J. L., Sollott, S. J., Der, C. J., Fearon, E. R., Sundaresan, M., Finkel, T., and Goldschmidt-Clermont, P. J. (1997) *Science 275*, 1649−1652.
53. Lander, H. M. (1997) *FASEB J. 11*, 118−124.
54. Brophy, P. M., and Barrett, J. (1990) *Biochem. Cell Biol. 68*, 1288−1291.

BI9804333